The Abdus Salam
International Centre for Theoretical Physics

United Nations
Educational, Scientific and
Cultural Organization

IAEA
International Atomic Energy Agency

2060-5

Advanced School on Non-linear Dynamics and Earthquake Prediction

28 September - 10 October, 2009

Inverse Retrospective Problems of Thermal Evolution of the Earth Interier: Applications

Alik T. Ismail-Zadeh
Geophysical Institute, University of Karlsruhe
Germany
International Institute of Earthquake Prediction Theory
Moscow
RUSSIAN FEDERATION

Alik.Ismail-Zadeh@gpi.uka.de

THE ABDUS SALAM
INTERNATIONAL CENTRE FOR THEORETICAL PHYSICS

Advanced School on
Non-linear Dynamics and Earthquake Prediction

28 September - 10 October 2009

INVERSE RETROSPECTIVE PROBLEMS OF THERMAL EVOLUTION OF THE EARTH INTERIOR:

APPLICATIONS

Alik T. Ismail-Zadeh

Geophysical Institute, University of Karlsruhe,
Hertzsrt. 16, Karlsruhe 76187, Germany.
E-mail: Alik.Ismail-Zadeh@gpi.uka.de

International Institute of Earthquake Prediction Theory and
Mathematical Geophysics, Russian Academy of Sciences,
84/32 Profsoyuznaya ul., Moscow 117997, Russia.

MIRAMARE-TRIESTE
2009

Earth and Planetary Science Letters 273 (2008) 68–79

Contents lists available at ScienceDirect

Earth and Planetary Science Letters

journal homepage: www.elsevier.com/locate/epsl

Thermal evolution and geometry of the descending lithosphere beneath the SE-Carpathians: An insight from the past

Alik Ismail-Zadeh [a,b,*], Gerald Schubert [c], Igor Tsepelev [d], Alexander Korotkii [d]

[a] Geophysikalisches Institut, Universität Karlsruhe, Hertzstr. 16, Karlsruhe 76187, Germany
[b] Institut de Physique du Globe de Paris, 4, Pl. Jussieu, Paris 75005, France
[c] Department of Earth and Space Sciences and Institute of Geophysics and Planetary Physics, University of California, 3806 Geology Building, 595 Charles Young Drive East, Los Angeles, CA 90095-1567, USA
[d] Institute of Mathematics and Mechanics, Ural Branch, Russian Academy of Sciences, S. Kovalevskoy ul. 16, Yekaterinburg 620219, Russia

A R T I C L E I N F O

Article history:
Received 2 November 2007
Received in revised form 5 June 2008
Accepted 11 June 2008
Available online 22 June 2008

Editor: T. Spohn

Keywords:
mantle dynamics
Vrancea
lithospheric slab
subduction
data assimilation

A B S T R A C T

Mantle heterogeneities imaged by seismic tomography in the SE-Carpathians contain information on the present thermal state of the mantle. Based on *P*-wave seismic velocity anomalies we develop a model of the present mantle temperature beneath the region and combine the model with a model of crustal temperature constrained by heat flow data. The modeled temperatures are assimilated into the geological past using the information on the regional movement in the Early and Middle Miocene. Prominent thermal states of the lithospheric slab descending in the region are restored from its diffuse present state. In Miocene times the slab geometry clearly shows two portions of the sinking body. The northwest–southeast oriented portion of the body is located in the vicinity of the boundary between the East European and Scythian platforms, and this portion of the sinking body may be a relic of cold lithosphere that has traveled eastward. Another portion has a northeast–southwest orientation and is related to the present descending slab. Above a depth of 60 km the slab had a concave thermal shape, confirming the curvature of the Carpathian arc, and a convex surface below that depth. The slab maintained its convex shape until it split into two parts at a depth of about 220 km. We propose that this change in the slab geometry, which is likely to be preserved until the present, can cause stress localization due to the slab bending and subsequent stress release resulting in large mantle earthquakes in the region. Also we hypothesize that either the processes of dehydration and partial melting of the descending lithospheric slab or dragging down of hotter rocks from the adjacent uppermost mantle by the slab are possible causes of the reduction in seismic velocities beneath the Transylvanian Basin.

1. Introduction

Repeated large intermediate-depth earthquakes in the southeastern (SE-) Carpathians (the Vrancea region) cause destruction in Bucharest, the capital city of Romania, and shake central and eastern European cities several hundred kilometers away from the hypocenters of the events. The earthquake-prone Vrancea region (Fig. 1) is bounded to the north and northeast by the Eastern European platform (EEP), to the east by the Scythian platform (SCP), to the south-east by the Focsani basin (FOC) and the North Dobrogea orogen (DOB), to the south and south-west by the Moesian platform (MOP), and to the north-west by the Transylvanian basin (TRB). The epicenters of the sub-crustal earthquakes in the Vrancea region are concentrated within a very small seismogenic volume about 70×30 km^2 in planform and between depths of about 70 and 180 km. Below this depth the seismicity ends abruptly: one seismic event at 220 km depth is an exception (Oncescu and Bonjer, 1997).

The 1940 $M_W = 7.7$ earthquake gave rise to the development of a number of geodynamic models for this region. McKenzie (1972) suggested that this seismicity is associated with a relic slab sinking in the mantle and now overlain by continental crust. The 1977 large earthquake and later the 1986 and 1990 earthquakes again raised questions about the nature of the earthquakes. A seismic gap at depths of 40–70 km beneath Vrancea led to the assumption that the lithospheric slab had already detached from the continental crust (Fuchs et al., 1979). Oncescu (1984) proposed that the intermediate-depth events are generated in a zone that separates the sinking slab from the neighboring immobile part of the lithosphere rather than in the sinking slab itself. Linzer (1996) explained the nearly vertical position of the Vrancea slab as the final rollback stage of a small fragment of oceanic lithosphere. Various types of slab detachment or delamination (e.g., Girbacea and Frisch, 1998; Wortel and Spakman, 2000; Gvirtzman, 2002; Knapp et al., 2005; Sperner et al., 2005) have been proposed to explain the present-day seismic images of the descending slab. Most recently Cloetingh et al.

* Corresponding author. Geophysikalisches Institut, Universität Karlsruhe, Hertzstr. 16, Karlsruhe 76187, Germany. Tel.: +49 721 6084610, +33 1 44272418; fax: +49 721 71173 (in GPI/UKA), +33 1 44273894 (in IPGP).
E-mail addresses: Alik.Ismail-Zadeh@gpi.uka.de, aiz@ipgp.jussieu.fr (A. Ismail-Zadeh), schubert@ucla.edu (G. Schubert), tsepelev@imm.uran.ru (I. Tsepelev), korotkii@imm.uran.ru (A. Korotkii).

0012-821X/$ – see front matter © 2008 Elsevier B.V. All rights reserved.
doi:10.1016/j.epsl.2008.06.012

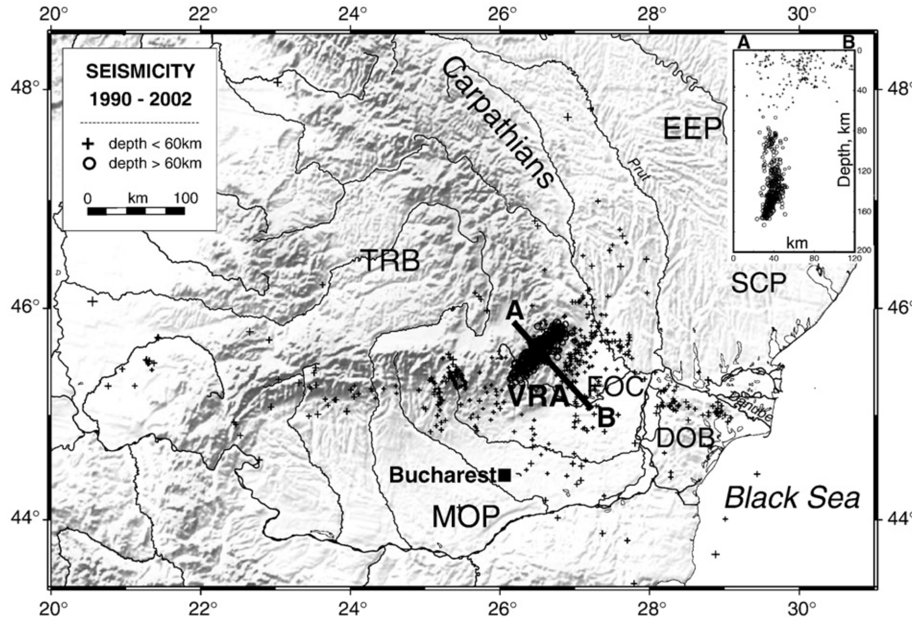

Fig. 1. Topography map of the SE-Carpathians and epicenters of Vrancea earthquakes (magnitude ≥ 3). Upper right panel presents hypocenters of the same earthquakes projected onto the NW–SE vertical plane AB. DOB, North Dobrogea orogen; EEP, Eastern European platform; FOC, Focsani basin; MOP, Moesian platform; SCP, Scythian platform; TRB, Transylvanian basin; and VRA, Vrancea.

(2004) argued in favor of the complex configuration of the underthrusted lithosphere and its thermo-mechanical age as primary factors in the behavior of the descending slab after continental collision. The origin of the descending lithosphere in the region, i.e., whether the Vrancea slab is oceanic or continental, is still under debate. Pana and Erdmer (1996) and Pana and Morris (1999) argued that because there is no geological evidence of Miocene oceanic crust in the eastern Carpathians, the descending lithosphere is likely to be thinned continental or transitional lithosphere.

The Neogene to Late Miocene (ca. 11 Myr) evolution of the Carpathian region is mainly driven by the northeastward, later eastward and southeastward rollback or slab retreat (Royden, 1988; Sperner et al., 2001) into a Carpathians embayment, consisting of the last remnants of an oceanic or thinned continental domain attached to the European continent (e.g., Balla, 1987; Csontos et al., 1992). When the mechanically strong Eastern European and Scythian platforms started to enter the subduction zone, the buoyancy forces of the thick continental crust exceeded the slab-pull forces and convergence stopped after only a short period of continental thrusting (Tarapoanca et al., 2004; Sperner et al., 2005). Continental convergence in the SE-Carpathians ceased about 11 Ma (Jiricek, 1979; Csontos et al., 1992), and after that the lithospheric slab descended beneath the Vrancea region due to gravity. The hydrostatic buoyancy forces promote the sinking of the slab, but viscous and frictional forces resist the descent. The combination of these forces produces shear stresses at intermediate depths that are high enough to cause earthquakes (Ismail-Zadeh et al., 2000, 2005b).

The principal aim of this paper is to present a quantitative model of the thermal evolution of the descending slab in the SE-Carpathians using a novel approach for assimilation of present crust/mantle temperature and flow in the geological past (Ismail-Zadeh et al., 2007). The model of the present temperature of the crust and upper mantle is estimated from body wave seismic velocity anomalies and heat flux data and is assimilated into Miocene times. We restore mantle thermal structures and analyze them in the context of modern regional geodynamics.

2. Present temperature model

Temperature is a key physical parameter controlling the density and rheology of the Earth's material and hence crustal and mantle dynamics. Besides direct measurements of temperature in boreholes in the shallow portion of the crust, there are no direct measurements of deep crustal and mantle temperatures, and therefore the temperatures must be estimated indirectly from seismic wave anomalies, geochemical data, and surface heat flow observations.

We develop a model of the present crustal and mantle temperature beneath the SE-Carpathians using the most recent high-resolution seismic tomography image (map of the anomalies of *P*-wave velocities) of the lithosphere and asthenosphere in the region (Martin et al., 2005, 2006). The tomography image shows a high-velocity body beneath the Vrancea region and the Moesian platform interpreted as the subducted lithospheric slab (Martin et al., 2006). The seismic–tomographic model of the region consists of eight horizontal layers of different thickness (15 km up to 70 km) starting from the depth of 35 km and extending down to a depth of 440 km. Each layer of about 1000×1000 km^2 is subdivided horizontally into 16×16-km^2 blocks. To restrict numerical errors in our data assimilation we smooth the velocity anomaly data between the blocks and the layers using a spline interpolation.

We follow the methodology by Ismail-Zadeh et al. (2005a) for the inference of temperature estimations from seismic wave anomalies and consider the effects of mantle composition, anelasticity, and partial melting on seismic velocities (see Appendix A). The temperature in the crust is constrained by measurements of surface heat flux corrected for paleoclimate changes and for the effects of sedimentation (Demetrescu et al., 2001).

Depth slices of the present temperature model are illustrated in Fig. 2. The pattern of resulting mantle temperature anomalies (predicted temperature minus background temperature) is similar to the pattern of observed *P*-wave velocity anomalies (Martin et al., 2006), but not an exact copy because of the nonlinear inversion of the seismic anomalies to temperature. The low temperatures are associated with the high-velocity body beneath the Vrancea region (VRA) and the East European platform (EEP) and are already visible at depths of 50 km. The slab image becomes clear at 70–110 km depth as a NE–SW oriented cold anomaly. With increasing depth (110–200 km depth) the thermal image of the slab broadens in NW–SE direction. The orientation of the cold body changes from NE–SW to N–S below the depth of 200 km. The slab extends down to 280–320 km depth beneath the Vrancea region itself. A cold anomaly beneath the Transylvanian

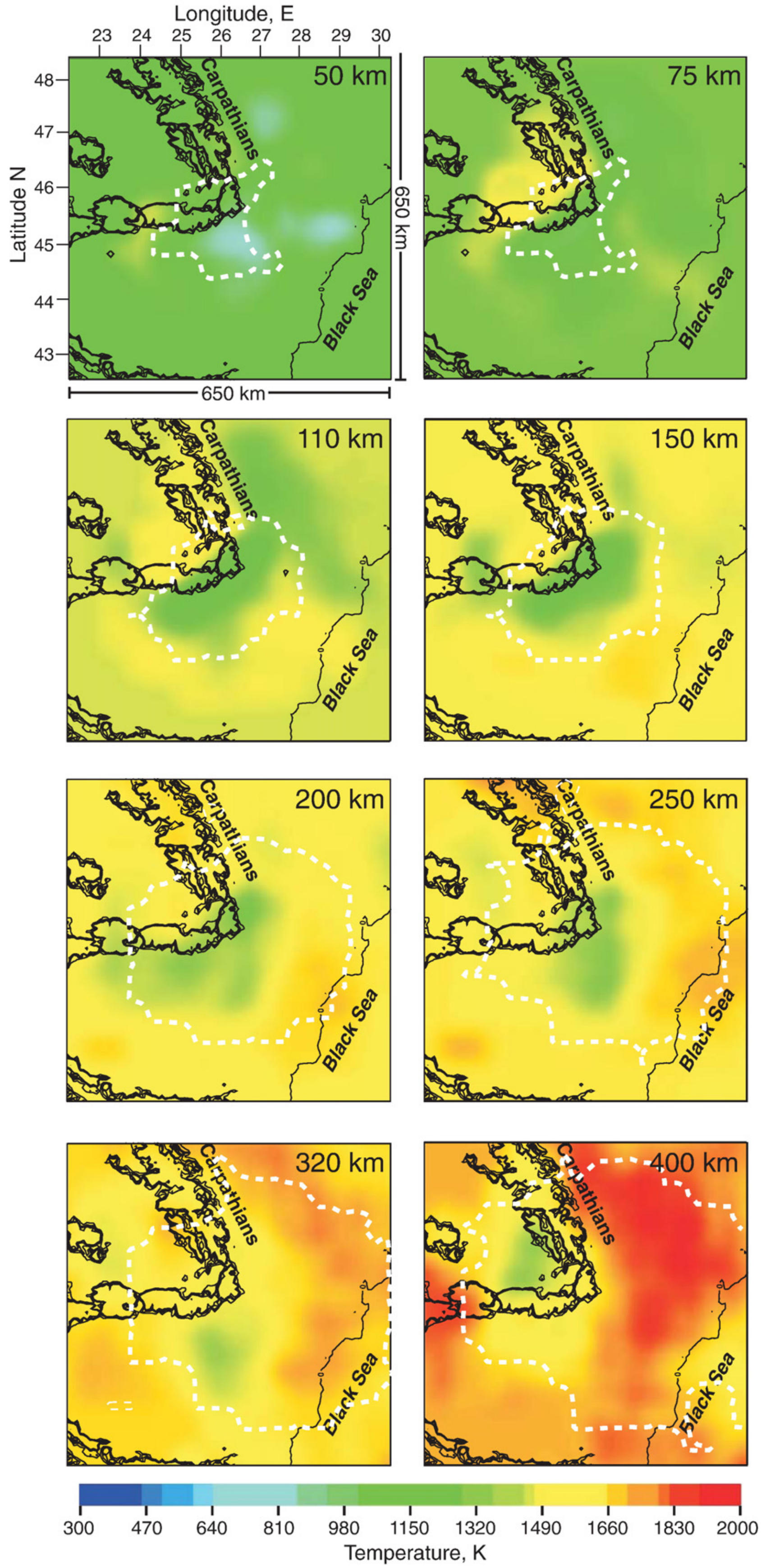

Fig. 2. Present temperature model as the result of the inversion of the *P*-wave velocity model. Theoretically well-resolved regions are bounded by dashed line (see text and Martin et al., 2006). Each slice presents a part of the horizontal section of the model domain Ω corresponding to $[x_1 = 177.5\text{ km}, x_1 = 825.5\text{ km}] \times [x_2 = 177.5\text{ km}, x_2 = 825.5\text{ km}]$, and the isolines present the surface topography (also in Figs. 3 and 5).

Table 1
Model parameters and values

Parameter	Symbol	Value
Horizontal dimensions	l_1, l_2 ($l_1=l_2$)	1005 km
Depth of domain	h	670 km
Acceleration due to gravity	g	9.8 m s^{-2}
Reference temperature	T_{ref}	2000 K
Surface temperature	T_{surf}	300 K
Temperature drop	$\Delta T = T_{ref} - T_{surf}$	1700 K
Thermal expansivity	α	3×10^{-5} K^{-1}
Thermal diffusivity	κ	10^{-6} m^2m^2 s^{-1}
Reference density	ρ_{ref}	3400 kg m^{-3}
Present time	ϑ	22 Myr
Reference viscosity	η_{ref}	10^{21} Pa s
Rayleigh number	Ra	5.2×10^5

Basin is estimated at depths of 370–440 km. According to Wortel and Spakman (2000) and Martin et al. (2006) this cold material can be interpreted as a remnant of subducted lithosphere detached during the Miocene along the Carpathian Arc and residing within the upper mantle transition zone. High temperatures are predicted beneath the Transylvanian Basin (TRB) at about 70–110 km depth. Two other high temperature regions are found at 110–150 km depth below the Moesian platform (MOP) and deeper than 200 km under the EEP and the North Dobrogea orogen (DOB), which might be correlated with the regional lithosphere/asthenosphere boundary.

3. Data assimilation

Data assimilation in geodynamical models can be defined as the incorporation of geophysical observations at present and initial physical conditions in the past into a dynamic quantitative model to provide time continuity and coupling among the geophysical fields (e.g., temperature, velocity). The basic principle of data assimilation is to consider the initial temperature in the geological past as a control variable and to optimize the initial temperature in order to minimize the discrepancy between the observations and the solution of the dynamic model (e.g., Ismail-Zadeh et al., 2003). The variational data assimilation was employed for numerical restoration of models of present prominent mantle plumes to their past stages (Ismail-Zadeh et al., 2004). The data assimilation allows recovering the crust and mantle structures prominent in the past from that weakened by thermal diffusion (Ismail-Zadeh et al., 2006).

To minimize boundary effects, the studied region (650×650 km^2 and 440 km deep, see Fig. 2) has been bordered horizontally by 200 km area and extended vertically to the depth of 670 km. Therefore we consider a rectangular three-dimensional (3-D) domain $\Omega=[0,x_1=l_1]\times[0,x_2=l_2]\times[0,x_3=h]$ for assimilation of present temperature and mantle flow beneath the SE-Carpathians. The momentum, continuity, and regularized backward heat equations in the Boussinesq approximation are solved numerically backward in time (Ismail-Zadeh et al., 2007):

$$\nabla P = \mathrm{div}[\eta(T)\mathbf{E}(\mathbf{u})] - RaT\boldsymbol{e}, \qquad \mathbf{x}\in\Omega \tag{1}$$

$$\mathrm{div}\mathbf{u} = 0, \qquad \mathbf{x}\in\Omega \tag{2}$$

$$\partial T/\partial t - \mathbf{u}\cdot\nabla T = \nabla^2 T - \beta\Lambda(\partial T/\partial t), \qquad t\in[0,\vartheta], \quad \mathbf{x}\in\Omega \tag{3}$$

with appropriate boundary conditions and the initial condition $T(\vartheta,\mathbf{x})=T_\vartheta(\mathbf{x})$. Here $\mathbf{x}=(x_1,x_2,x_3)$, $\mathbf{u}=(u_1,u_2,u_3)$, t, T, P, and η are the dimensionless Cartesian coordinates, velocity, time, temperature, pressure, and viscosity, respectively; $\boldsymbol{e}=(0,0,1)$ is the unit vector; $\mathbf{E}=e_{ij}(\mathbf{u})=\{\partial u_i/\partial x_j+\partial u_j/\partial x_i\}$ is the strain rate tensor; ∇ is the gradient operator; div is the divergence operator; $[t=0,\ t=\vartheta]$ is the assimilation time interval; $\Lambda(T)=\partial^4T/\partial x_1^4+\partial^4T/\partial x_2^4+\partial^4T/\partial x_3^4$, $\beta>0$ is the regularization parameter; and $T_\vartheta(\mathbf{x})$ is the known temperature at present time $t=\vartheta$. The Rayleigh number is defined as $Ra=\alpha g\rho_{ref}\Delta T h^3\eta_{ref}^{-1}\kappa^{-1}$. Length, temperature, and time are normalized by h, ΔT, and $h^2\kappa^{-1}$, respectively. The physical parameters of the fluid (temperature, velocity, pressure, viscosity, and density) are assumed to depend on time and on space coordinates. Parameters used in the modeling are listed in Table 1. We consider a temperature-dependent Newtonian rheology for the crust and mantle, although the mantle rocks exhibit more complex rheological properties:

$$\eta = \eta_{ref}\exp(Q/(T/T_{ref}+G) - Q/(0.5+G)), \tag{4}$$

where $Q=[225/\ln(r)]-0.25\ln(r)$, $G=15/\ln(r)-0.5$, and $r=1000$ is the ratio between the viscosity on the upper and lower boundary of the model domain (Busse et al., 1993).

Our ability to reverse mantle flow is limited by our knowledge of past movements in the region, which are well constrained only in some cases. In reality, the Earth's crust and lithospheric mantle are driven by mantle convection and the gravitational pull of dense descending slabs. However, when a numerical model is constructed for a particular region, external lateral forces can influence the regional crustal and uppermost mantle movements. Yet in order to make useful predictions that can be tested geologically, a time-dependent numerical model

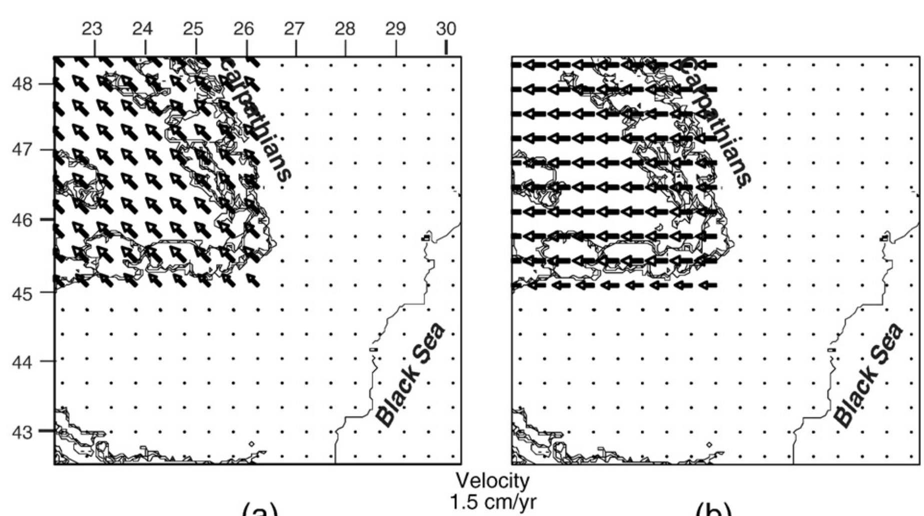

Fig. 3. Surface velocity imposed on the part of the upper boundary of the model domain (see the caption of Fig. 2) in data assimilation modeling for the time interval from 11 Myr to 16 Myr ago (a) and for that from 16 Myr to 22 Myr ago (b).

should include the history of surface motions. Since this is not currently achievable in a dynamical way, it is necessary to prescribe surface motions using velocity boundary conditions.

The simulations are performed backward in time for a period of 22 Myr. We assume perfect slip conditions at the vertical and lower boundaries of the model domain. For the first 11 Myr (starting from the present time), when the rates of continental convergence were insignificant (Jiricek, 1979; Csontos et al., 1992), no velocity is imposed at the surface, and the conditions at the upper boundary are free slip. We impose the northwestward velocity in the portion of the upper model boundary (Fig. 3a) for the time interval from 11 Myr to 16 Myr and westward velocity in the same portion of the boundary (Fig. 3b) for the interval from 16 Myr to 22 Myr. The velocities are consistent with the direction and rates of the regional convergence in the Early and Middle Miocene (Morley, 1996; Fügenschuh and Schmid, 2005; Sperner et al., 2005). The effect of the surface loading due to the Carpathian Mountains is not considered, because this loading would have insignificant influence on the dynamics of the region (as was shown in two-dimensional models of the Vrancea slab evolution; Ismail-Zadeh et al., 2005b).

The heat flux through the vertical boundaries of the model domain is set to zero. The upper and lower boundaries are assumed to be isothermal surfaces. The present temperature above 440 km depth is derived from the seismic velocity anomalies and heat flow data. We use the adiabatic geotherm for a potential temperature 1750 K (Katsura et al., 2004) to define the present temperature below 440 km (where seismic tomography data are not available).

Eqs. (1)–(4) with the prescribed boundary and initial conditions are solved numerically by the Eulerian spline finite-element and finite-difference methods. The reader is referred to Ismail-Zadeh et al. (2001) for details of numerical solvers and to Ismail-Zadeh et al. (2007) for details of the numerical approach to data assimilation (see also Appendix B).

To estimate the accuracy of the results of data assimilation, we employ the temperature and mantle flow restored to the time of 22 Myr ago as the initial condition for a model of the slab evolution forward in time, run the model to the present, and analyze the temperature residual (the difference between the present temperature and that predicted by the forward model with the restored temperature as an initial temperature distribution). The maximum temperature residual does not exceed 50°.

A sensitivity analysis was performed to understand how stable is the numerical solution to small perturbations of input (present) temperatures. The model of the present temperature (Section 2) has been perturbed randomly by 0.5 to 2% and then assimilated to the past to find the initial temperature. A misfit between the initial temperatures related to the perturbed and unperturbed present temperature is rather small (2 to 4%) which proves that the solution is stable.

The numerical models, with a spatial resolution of 7 km × 7 km × 5 km, were run on parallel computers. The accuracy of the numerical solutions has been verified by several tests, including grid and total mass changes (Ismail-Zadeh et al., 2001) and comparison with the analytical solution to the 3-D Stokes equation combined with the equation for advection of temperature (Trushkov, 2002).

4. What the past tells us

We assimilate the present temperature model into Miocene times to restore the prominent thermal features of the lithospheric slab in the SE-Carpathians. Although there is some evidence that the slab was already partly subducted some 75 Myr ago (e.g., Sandulescu, 1988), the assimilation interval is restricted in this study to the Miocene, because the pre-Miocene evolution of the descending slab, as well as the regional horizontal movements, are poorly known. Incorporation of insufficiently accurate data into the assimilation model could result in incorrect scenarios of mantle and lithosphere dynamics in the region. Moreover, to restore the history of pre-Miocene slab subduction, a high-resolution seismic tomography image of the deeper mantle is required (the present image is restricted to the depth of 440 km). Therefore, we have avoided assimilation of the data beyond Miocene time.

Early Miocene subduction beneath the Carpathian arc and the subsequent gentle continental collision transported cold and dense lithospheric material into the hotter mantle. Fig. 4 presents the 3-D thermal image of the slab and pattern of contemporary flow induced by the descending slab. Note that the direction of the flow is reversed, because we solve the problem backward in time: cold slab move upward during the numerical modeling. The 3-D flow is rather complicated: toroidal (in horizontal planes) flow at depths between about 100 to 200 km coexists with poloidal (in vertical planes) flow.

The relatively cold (blue to dark green) region seen at depths of 40 km to 230 km (Fig. 5b–d) can be interpreted as the earlier evolutionary stages of the lithospheric slab. The slab is poorly visible at shallow depth in the model of the present temperature (Fig. 5a). Since active subduction of the lithospheric slab in the region ended in

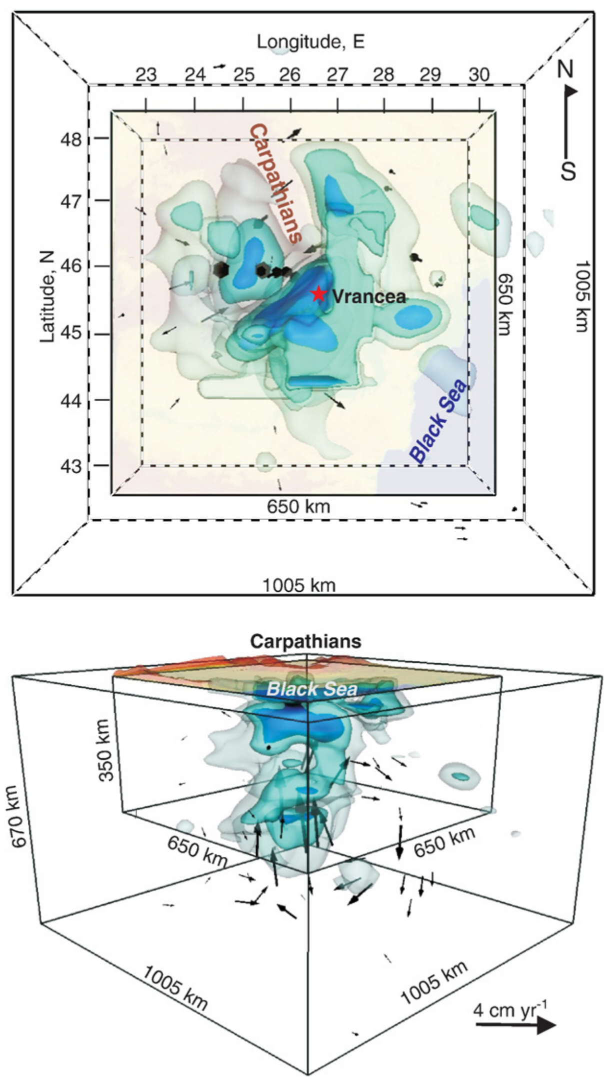

Fig. 4. 3-D thermal shape of the Vrancea slab and contemporary flow induced by the descending slab beneath the SE-Carpathians. Upper panel: top view. Lower panel: side view from the SE toward NW. Arrows illustrate the direction and magnitude of the flow. The marked sub-domain of the model domain presents the region around the Vrancea shown in Fig. 5 (in horizontal slices) and in Fig. 6. The surfaces marked by blue, dark cyan, and light cyan illustrate the surfaces of 0.07, 0.14, and 0.21 temperature anomaly δT, respectively, where $\delta T = (T_{hav} - T)/T_{hav}$, and T_{hav} is the horizontally averaged temperature. The top surface presents the topography, and the red star marks the location of the intermediate-depth earthquakes.

Late Miocene time and earlier rates of convergence were low before it, we argue that the cold slab, descending slowly at these depths, has been warmed up, and its thermal shape has faded due to heat diffusion. Thermal conduction in the shallow Earth (where viscosity is high) plays a significant part in heat transfer compared to thermal convection. The deeper we look in the region, the larger are the effects of thermal advection compared to conduction: the lithosphere has moved upwards to the place where it had been in Miocene times. Below 230 km depth the thermal roots of the cold slab are clearly visible in the present temperature model (Figs. 2, 4, and 5a), but they are almost invisible in Fig. 5b–d and in Fig. 6 of the models of the assimilated temperature, because the slab did not reach these depths in Miocene times.

The geometry of the restored slab clearly shows two parts of the sinking body (Figs. 5b–d and 6). The NW–SE oriented part of the body is located in the vicinity of the boundary between the EEP and Scythian platform (SCP) and may be a relic of cold lithosphere that has traveled eastward. Another part has a NE–SW orientation and is associated with the present descending slab. An interesting geometrical feature of the restored slab is its curvature beneath the SE-Carpathians. In Miocene times the slab had a concave surface confirming the curvature of the Carpathian arc down to depths of about 60 km. At greater depths the slab changed its shape to that of a convex surface and split into two parts at a depth of about 200 km. Although such a change in slab curvature is visible neither in the model of the present temperature nor in the seismic tomography image most likely because of slab warming and heat diffusion, we suggest that the convex shape of the slab is likely to be preserved at the present time. We argue that this change in the geometry of the descending slab can cause stress localization due to slab bending and subsequent stress release resulting in earthquakes, which occur at depths of 70 to 180 km in the region.

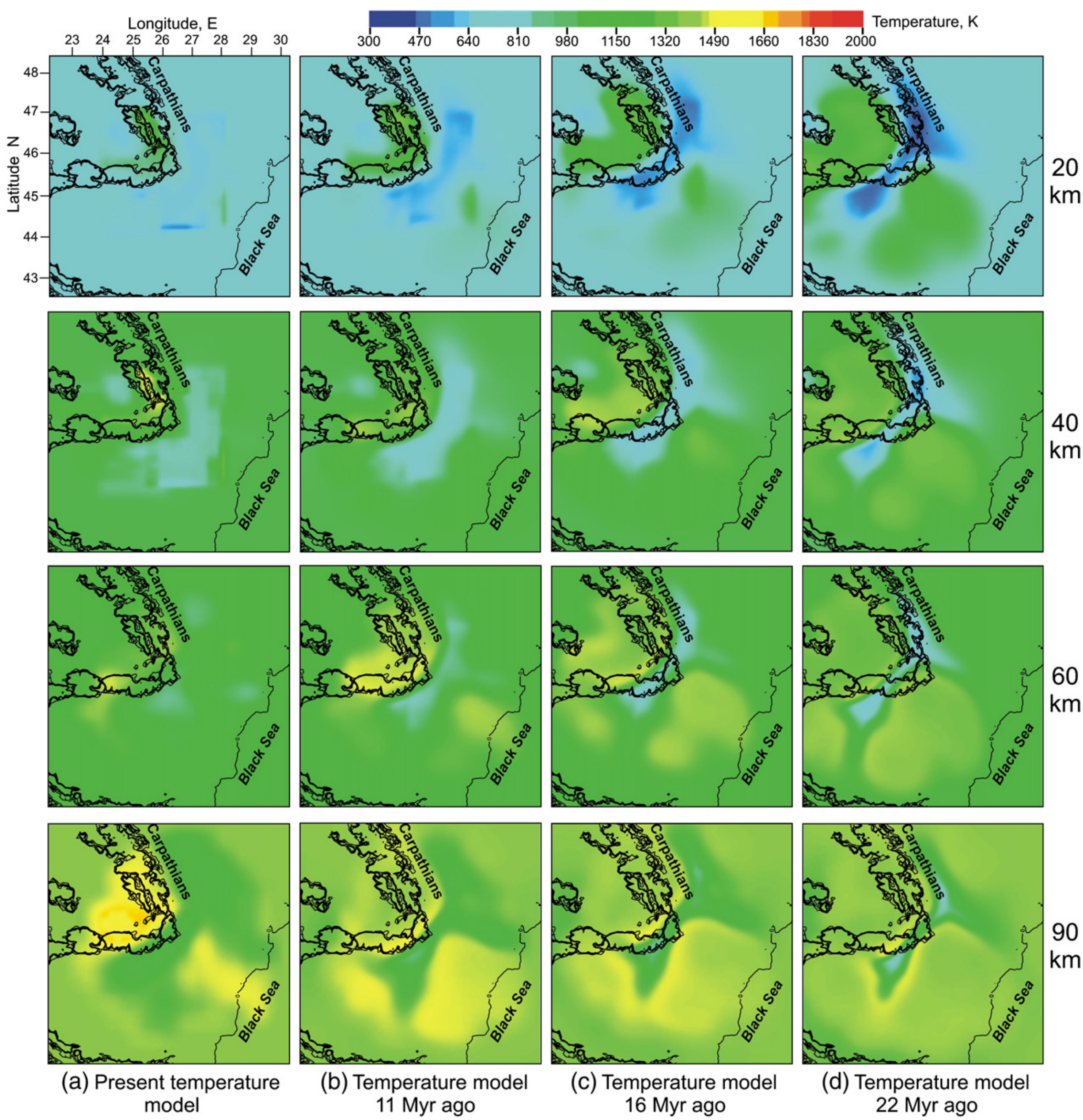

Fig. 5. Thermal evolution of the crust and mantle beneath the SE-Carpathians. Horizontal sections of temperature obtained by the assimilation of the present temperature (a) to the Miocene times (b–d).

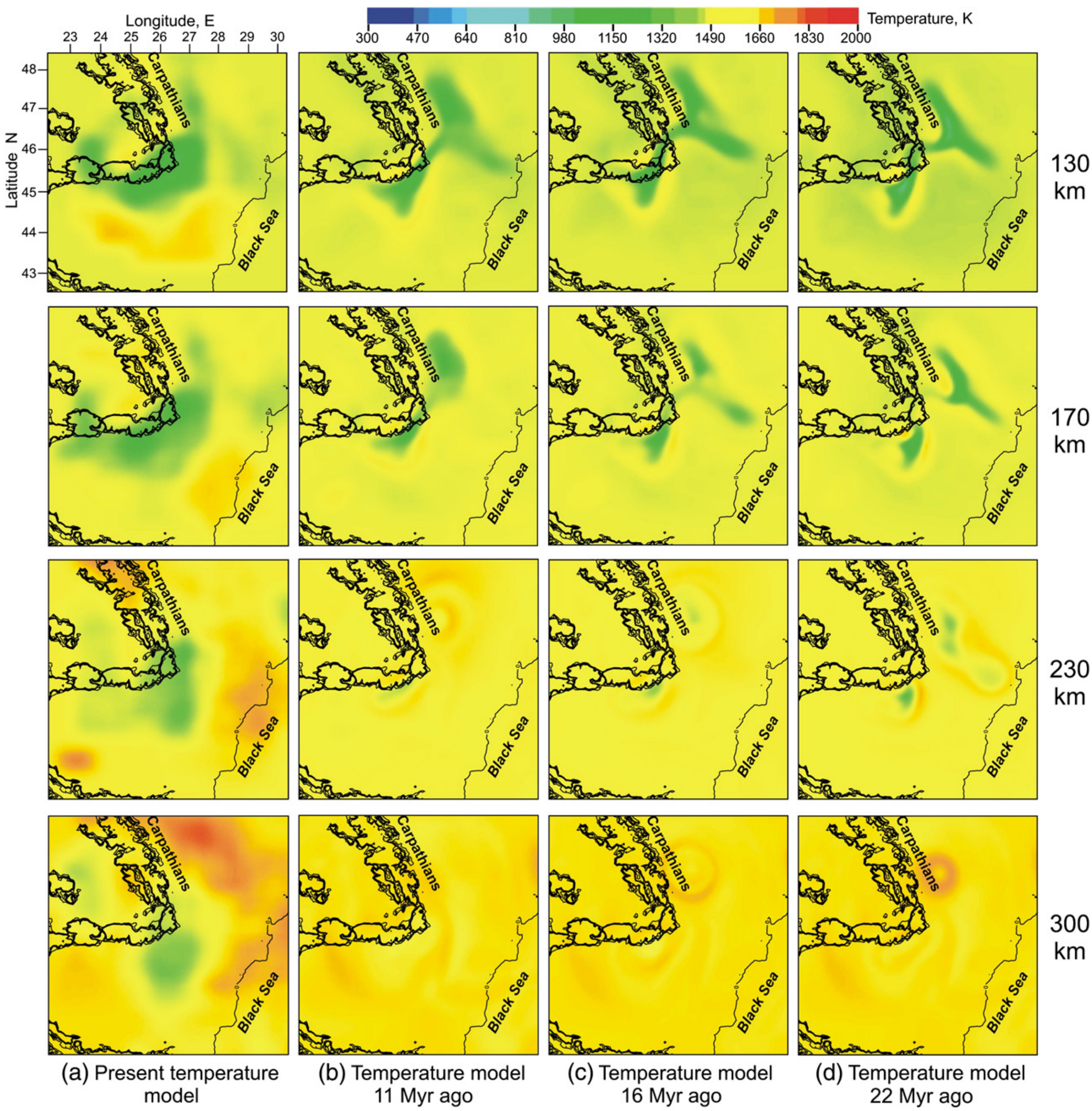

Fig. 5 (*continued*).

Moreover, the north-south (NS)-oriented cold material visible at the depths of 230 km to 320 km (Figs. 2 and 5a) does not appear as a separate (from the NE–SW-oriented slab) body in the models of Miocene time. Instead, it looks more like two differently oriented branches of the SW-end of the slab at 60–130 km depth (visible in Figs. 5b–d and 6). Therefore, the results of the assimilation of the present temperature model to Miocene time provide a plausible explanation for the change in the spatial orientation of the slab from NE–SW to NS beneath 200 km observed in the seismic tomography image (Martin et al., 2006).

The slab bending might be related to a complex interaction between two parts of the sinking body and the surrounding mantle. The sinking body displaces the mantle, which, in its turn, forces the slab to deform due to corner (toroidal) flows different within each of two sub-regions (to NW and to SE from the present descending slab). Also, the curvature of the descending slab can be influenced by slab heterogeneities due to variations in its thickness and viscosity (Cloetingh et al., 2004; Morra et al., 2006).

According to Roure et al. (1993) and Fügenschuh and Schmid (2005), the trench (hence, the location of the subduction zone) migrated towards the east and southeast over a distance of 160–180 km since the Miocene times. The NW–SE vertical section across the SE-Carpathians illustrates the modeled descending slab (light to dark blue) at the present time (Fig. 7a) and its restored positions in the geological past (Fig. 7b–d). Besides deepening into the mantle, the descending slab in the model traveled for 22 Myr over a distance of at least 160 km toward the northeast. The slab geometry shows that the restored slab is laterally thin compared to the present thick slab (Fig. 7; also compare the slab images in Figs. 4–6). This can be explained by the fact that a slab descending into the mantle thickens with depth and develops a 'tear-shaped' structure of lithospheric material with time (e.g., Ismail-Zadeh et al., 2005b).

The Neogene–Middle Miocene tectonic evolution of the SE-Carpathians is considered by Sperner et al. (2001) to be influenced by west-dipping subduction (according to the thrusting direction of the accretionary wedge) beneath the inner-Carpathian block. These

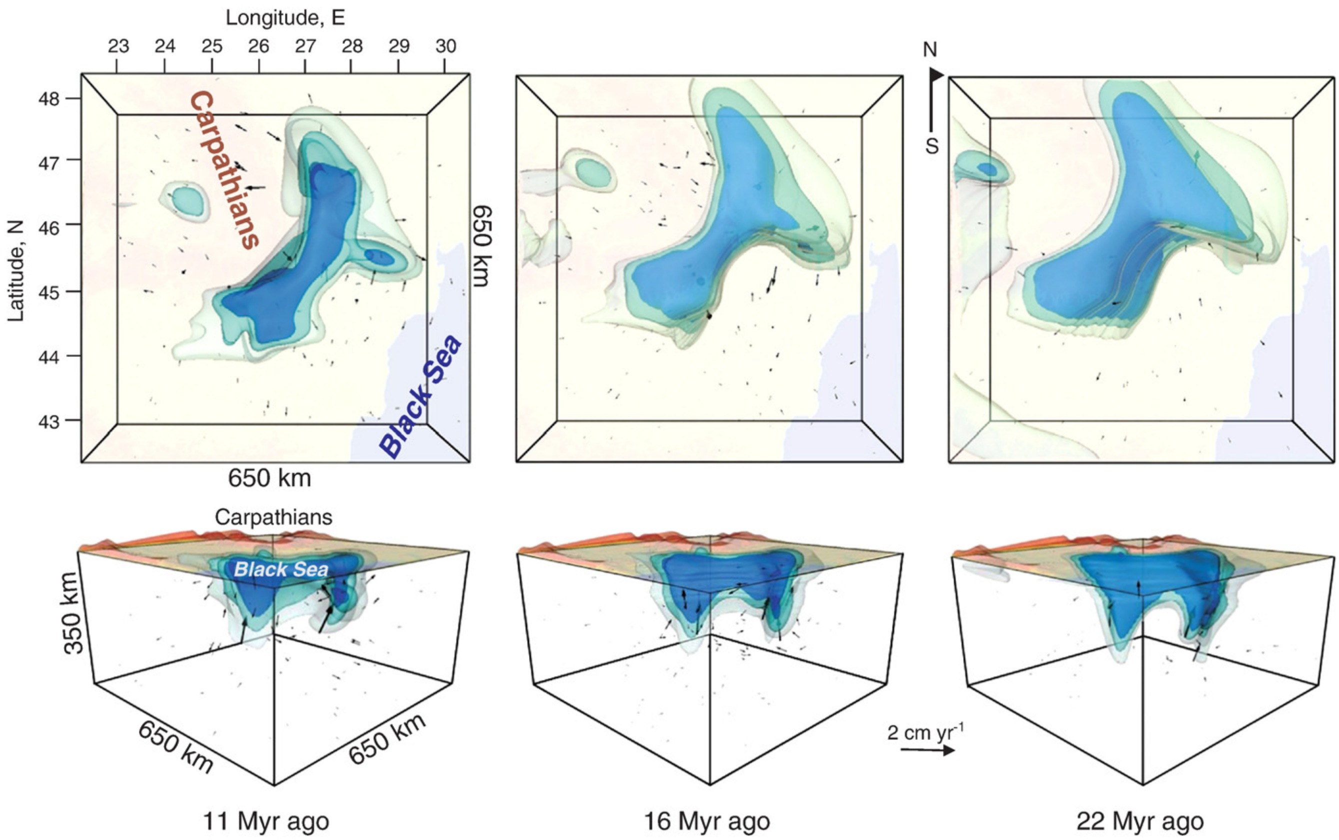

Fig. 6. Snapshots of the 3-D thermal shape of the Vrancea slab and pattern of mantle flow beneath the SE-Carpathians in the Miocene times. See Fig. 4 for other notations.

authors believe that the velocity of the oceanic slab subduction was larger than the convergence velocity, and this resulted in the slab retreat toward the east and in the eastward movement of the inner-Carpathian block.

The results of our quantitative model show the restored slab positions in the Miocene times and suggest an alternative scenario for the slab evolution. The east-dipping part of the slab (dark blue in Fig. 7c, d) subducted beneath the SE-Carpathians toward the older west-dipping subduction zone (dark green at the center of Fig. 7c, d). The east-dipping slab descent continued until the collision between the inner-Carpathian lithosphere and the East European platform in the Late Miocene. The modeled mantle-lithosphere dynamics in the SE-Carpathians illustrates a retreat of the descending lithosphere toward the east and the southeast due to extension in the Pannonian basin.

The subsequent evolution of the Vrancea slab was controlled by the slab buoyancy. Based on the correlation between the position of sediments depocenters in the Focsani basin, the Vrancea seismicity, and the high-velocity body imaged by seismic tomography, Matenco et al. (2007) showed that the Late Miocene–Pliocene subsidence in the region was driven by the Vrancea slab-pull. Our scenario for the Miocene evolution of the descending Vrancea slab explains the slab shift toward the southeast by about 160 km in the Early–Middle Miocene times and the accumulation of the thick post-collisional sediments in the Focsani basin due to the slab-pull.

Martin et al. (2006) interpret the negative velocity anomalies NW of the present slab at depths between 70 and 110 km (see the relevant temperature slices in Figs. 2, 5a, and 7a) as a shallow asthenospheric upwelling associated with possible slab rollback. Also, they mention partial melting as an additional contribution to the reduction of seismic velocities at these depths. The results of our assimilation show that the descending slab is surrounded by a border of hotter rocks at depths down to about 250 km (Fig. 7). The rocks could be heated due to partial melting as a result of slat dehydration. Although we do not consider the effects of slab dehydration or partial melting in the modeling, the numerical results support the hypothesis of dehydration of the descending lithosphere and its partial melting as the source of reduction of seismic velocities at these depths and probably deeper (see temperature slices at the depths of 130 to 220 km). Alternatively, the hot anomalies beneath the Transylvanian basin and partly beneath the Moesian platform (see Fig. 7d) could be dragged down by the descending slab since the Miocene times, and therefore, the slab was surrounded by the hotter rocks (Fig. 7a–c). Using numerical experiments Honda et al. (2007) showed recently how the lithospheric plate subducting beneath the Honshu Island in Japan dragged down a hot anomaly adjacent to the plate.

Some areas of high temperature at depths below 280 km can be associated with mantle upwelling in the region. High-temperature anomalies are not clearly visible in the restored temperatures at these depths, because the upwelling was likely not active in Miocene times.

5. Uncertainties and limitations in data assimilation

There are at least two sources of error in data assimilation (apart from the errors associated with the numerical modeling): data misfit related to the uncertainties in the present temperature distribution and/or in the surface movements and errors due to the uncertainties in initial and boundary conditions.

Many models of mantle temperature are based on the conversion of seismic tomography data. The key to an appropriate interpretation of seismic velocity anomalies in tomographic studies is a detailed resolution analysis. Martin et al. (2006) studied the theoretical resolution of their tomography model for the SE-Carpathians by analyzing the resolving width (RW) functional. The RW functional presents the quality of the resolution for the velocity at predefined nodes: its values decrease for

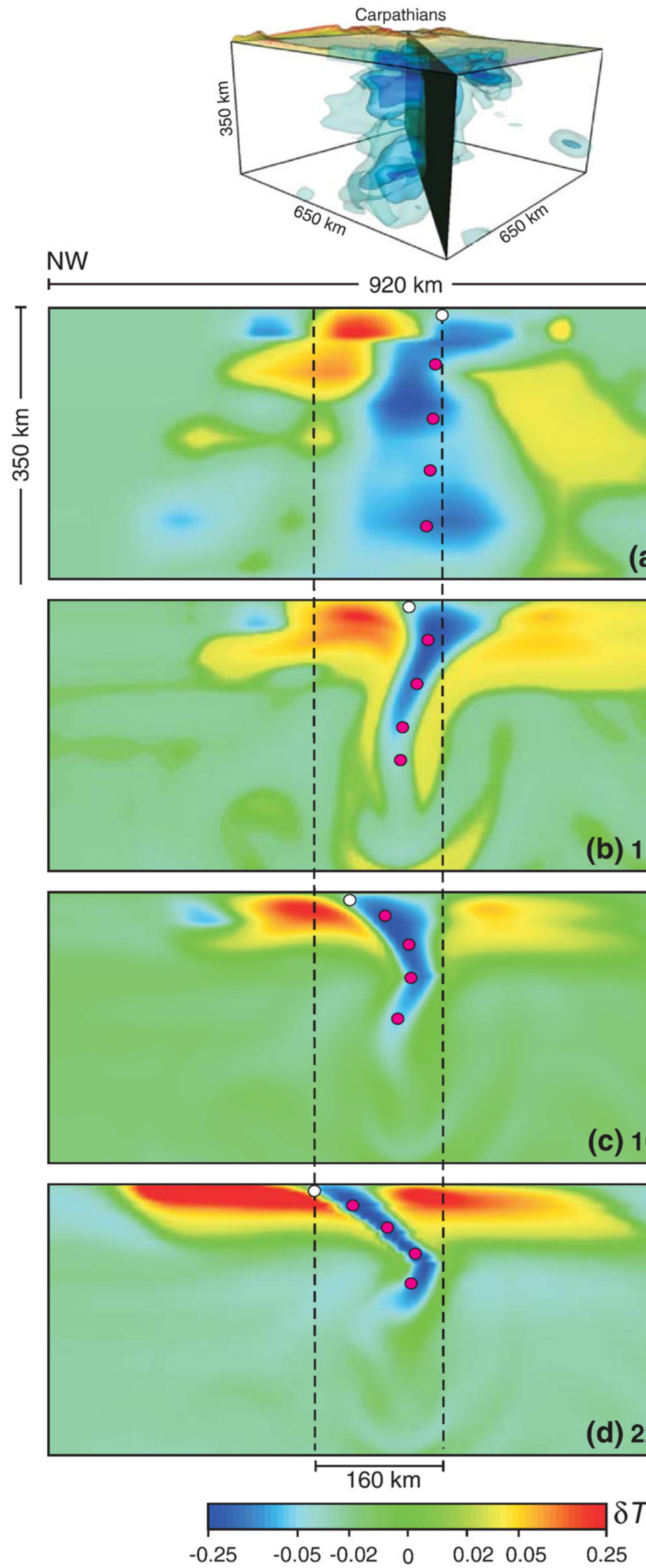

Fig. 7. Thermal evolution of the descending Vrancea slab since the Miocene times. Temperature anomalies δT defined in the caption of Fig. 4 are presented in the NW–SE vertical section (see the upper panel for the section's location). Circles show the location of the passive markers incorporated in the numerical model to display the slab movement. The white circle presents the location of the modeled subduction zone.

well-resolved nodes and increase with the amount of smearing. Fig. 2 presents the areas, bounded by the white contour lines, where the values of the RW functional do not exceed 4.0 (compared to 2.0 in the best case and 8.0 in the worth case of the tomography resolution). Therefore, the results of temperature conversion from the seismic tomography model of Martin et al. (2006) should be reliable enough, at least in the areas of high tomography resolution.

There is a major physical limitation of the restoration of mantle structures. If a thermal feature created, let us say, hundreds million years ago has completely diffused away by the present, it is impossible to restore the feature, which was more prominent in the past. The time to which a present thermal structure in the upper mantle can be restored should be restricted by the characteristic thermal diffusion time, the time when the temperatures of the evolved structure and the ambient mantle are nearly indistinguishable (Ismail-Zadeh et al., 2004).

The time (t) for restoration of seismic thermal structures depends on depth (d) of seismic tomography images and can be roughly estimated as $t=d / v$, where v is the average vertical velocity of mantle flow. For example, the time for restoration of the Vrancea slab evolution in the studied models should be less than about 80 Myr, considering $d=$ 400 km and $\nu\approx 0.5$ cm yr^{-1}.

Other sources of uncertainty in the modeling of mantle temperature come from the choice of mantle composition (Nitoi et al., 2002; Seghedi et al., 2004; Szabo et al., 2004), the seismic attenuation model (Popa et al., 2005; Weidle et al., 2007), and poor knowledge of the presence of water at mantle depths. The drop of electrical resistivity below 1 Ω m (Stanica and Stanica, 1993) can be an indicator of the presence of fluids (due to dehydration of mantle rocks) below the SE-Carpathians; however, the information is very limited and cannot be used in quantitative modeling. Therefore, if the present mantle temperature model is biased, the information can be improperly propagated to the geological past.

The conditions at the boundaries of the model domain used in the data assimilation are, of course, an approximation to the real temperature, heat flux, and movements, which are practically unknown and, what is more important, may change over time at these boundaries. The results of data assimilation will hence depend on the model boundary conditions. Moreover, errors associated with the knowledge of the temperature (or heat flux) evolution or of the regional horizontal surface movements can propagate into the past during data assimilation.

Viscosity is an important physical parameter in numerical modeling of mantle dynamics, because it influences the stress state and results in strengthening or weakening of Earth's material. Though it is the least-known physical parameter of the model, the viscosity of the Vrancea slab was constrained by observations of the regional strain rates. Intermediate-depth earthquakes in the Vrancea region provide an indirect measure of the rate of strain release within the seismogenic body (8×10^{18} N m yr^{-1}, Ismail-Zadeh et al., 2000). The strain rate (ratio between stress and viscosity), as a result of the Vrancea earthquakes, was estimated to be 7.5×10^{-15} s^{-1} (Wenzel et al., 1999). This strain rate was used as a constraint on the viscosity of the model slab in our test computations of the flow (and strain rate) for various viscosity ratios between slab and mantle. Based on these tests, we adopted the background viscosity η_{ref} to be 10^{21} Pa s.

Though interpretation of seismic tomography in terms of temperature and temperature assimilation are somewhat uncertain, we believe that data assimilation is useful for improving our understanding of the thermal and dynamic evolution of the Earth's crust and mantle. New high-resolution experiments on seismic wave attenuation, improved knowledge of crustal and mantle mineral composition, accurate GPS measurements of regional movements, and precise geological paleoreconstructions of crustal movements in the SE-Carpathians will help refine the present model and our knowledge of the regional thermal evolution.

6. Conclusion

The origin of large intermediate-depth earthquakes in the SE-Carpathians is still under debate. Several processes can contribute to the stress generation and its release in the Vrancea region. Among the processes are buoyancy, viscous and frictional forces (Ismail-Zadeh et al., 2000; 2005a,b), plastic instability at high temperature (Griggs and Baker, 1969), faulting due to metamorphic phase transitions (Green and Burnley, 1989; Ismail-Zadeh et al., 2000), and dehydration-induced embrittlement (Ismail-Zadeh et al., 2000; Hacker et al., 2003). We have suggested here that bending forces can contribute to the stress field of the descending lithosphere in the SE-Carpathians.

The images of the restored earlier stages of the thermal evolution of the mantle in the region show that the descending lithospheric slab changes its curvature from a concave to convex shape, and the area of the maximum bending coincides with the area of intermediate-depth Vrancea earthquakes. A concentration of earthquakes associated with slab bending is also seen in other subduction zones, most prominently at the Fiji end of the Tonga slab (Chen and Brudzinski, 2001).

The negative seismic velocity anomalies and high temperatures beneath the Transylvanian basin (TRB) are likely associated either with the processes of dehydration and partial melting of rocks in the descending lithosphere or with dragging down of hotter rocks from the adjacent uppermost mantle, rather than with slab rollback and subsequent asthenospheric upwelling. An analysis of high-resolution seismic wave attenuation and P- and S-wave seismic tomography images combined with mineral physics can provide estimates of water and melt contents in the region.

Using data assimilation we have shown that the geometry of the mantle structures changes with time, diminishing the degree of surface curvature of the structures. Like Ricci flow, which tends to diffuse regions of high curvature into ones of lower curvature (Hamilton, 1982; Perelman, 2002), heat conduction smoothes the complex thermal surfaces of mantle bodies with time. Present seismic tomography images of mantle structures do not allow definition of the sharp shapes of these structures. Assimilation of mantle temperature and flow to the geological past instead provides a quantitative tool to restore thermal shapes of prominent structures in the past from their diffusive shapes at present.

Acknowledgments

The authors are very grateful to S. Cloetingh, D. Pana, and an anonymous reviewer for constructive comments on the initial version of this paper, to S. Honda, S. Sobolev, and B. Sperner for discussions on the regional geology and data assimilation, and to M. Martin and F. Wenzel for the seismic tomography data of the Vrancea region made available for the research. This work was supported by the German Research Foundation, French-Russian Collaboration Program, Russian Academy of Sciences, and Russian Foundation for Basic Research.

Appendix A. Inversion of *P*-wave seismic velocity anomalies into temperature

Non-linear teleseismic body wave tomography with data of the 1999 Carpathian Arc Lithosphere X-Tomography experiment in Romania provides high-resolution imaging of the upper mantle structure (Martin et al., 2006). 194 teleseismic events are used for the seismic tomography study in the SE-Carpathians. All data were recorded at the 110 seismic stations (including 24 broad-band stations with a sampling rate ≥50 Hz in the field), which were located densely around the Vrancea region. All seismograms were bandpass filtered between 0.5–2 Hz to enhance the suitable phases *P* and *PKP*, and all earthquake hypocenters were taken from the relocated earthquake catalogue of Engdahl et al. (1998). Source effects and path effects between source and model are effectively removed in teleseismic tomography by using weighted relative residuals for each event (e.g., Evans and Achauer, 1993). Smearing from strong crustal velocity anomalies into the upper mantle was suppressed by travel-time corrections with a priori three-dimensional regional crustal velocity model (Martin et al., 2005). Travel-time residuals were calculated relative to the IASP91 earth model (Kennett and Engdahl, 1991).

The seismic velocity anomalies in the upper mantle can be attributed to variations in temperature (Forte et al., 1994, 1995), although several factors other than temperature can also exert an influence on seismic velocity, e.g., composition (Griffin et al., 1998), anelasticity (Karato, 1993), and presence of melt or water (Karato, 2004). Therefore, in the forward modeling of synthetic *P*-wave seismic velocity anomalies beneath the SE-Carpathians we consider the effects of anharmonicity (composition), anelasticity and partial melting on seismic velocities.

The anharmonic (frequency independent and non-attenuating) part of the synthetic velocities is calculated on the basis of published data on laboratory measurements of density and elastic parameters of the main rock-forming minerals (Bass, 1995) at various thermodynamic conditions. We accept the following model of a composite mineralogy: 57.9% Ol, 16.3% CPx, 13.5% Opx, and 12.3% Gt for the crust and mantle (Green and Falloon, 1998) and 69% Ol, 10% CPx, 19% Opx, and 2% Gt for the slab (Agee, 1993). For each single mineral constituting the models of crust/mantle composition density ρ, thermal expansivity α, the elastic bulk modulus K and shear modulus μ and their pressure and temperature derivatives should be estimated at an ambient condition (T_0, P_0) to determine the anharmonic part of the velocity V_{anh} depending on temperature T and pressure P (Goes et al., 2000).

Viscoelastic relaxation at high temperature leads to frequency dependence of seismic wave velocities and attenuation of seismic waves (e.g., Kanamori and Anderson, 1977; Karato, 1993). Shear anelasticity in minerals at high temperatures and low frequencies can be represented by the following relationship: $Q_\mu(\omega,P,T)=B\omega^a\exp\left(\frac{aH}{RT}\right)$, where the Q-factor is defined as the ratio of elastic energy stored in a system to the energy loss per unit cycle, B (=0.148) is a normalization factor, ω (=1 Hz) is the frequency, a (=0.15) is the exponent describing the frequency dependence of the attenuation, H (=5×10^5 J mol^{-1}) is the activation enthalpy, and R is the universal gas constant. The values for B, a, and H are based on various experimental data (e.g., Karato, 2004). The frequency is consistent with the seismic frequency of PREM (Dziewonski and Anderson, 1981) and AK135 (Montagner and Kennett, 1996). Therefore, the synthetic velocity V_{syn} accounting for the anelasticity can be calculated as

$$V_{\text{syn}}(P,T)=V_{\text{anh}}(P,T)\left[1-\frac{Q^{-1}(\omega,P,T)}{2\tan(\pi a/2)}\right],$$

where $Q^{-1}=(1-L)Q_K^{-1}+LQ_\mu^{-1}$, $L=4V_S^2/3V_P^2$, and Q_K=57,822 (Dziewonski and Anderson, 1981). Once the synthetic velocities are calculated for a first-guess temperature, an iteration process is used to find the temperature $T^n=T_{\text{bg}}+\delta T^n$, minimizing the difference between the synthetic $\delta V_{\text{syn}}=(V_{\text{syn}}(P,T_{\text{bg}})-V_{\text{syn}}(P,T))/V_{\text{syn}}(P,T_{\text{bg}})$ and 'observed' δV_{obs} (in seismic tomography experiments) velocity anomalies:

$$\delta T^{n+1}=\delta T^n+F_{\text{d}}\left(\delta V_{\text{obs}}-\delta V_{\text{syn}}\right)\Big/\frac{\partial V_{\text{syn}}}{\partial T}\to\min_T \qquad \text{at} \qquad T<T_{\text{sol}},$$

$$\delta T^{n+1}=\delta T^n+F_{\text{d}}\left(\delta V_{\text{obs}}-\delta V_{\text{syn}}-\frac{\partial V_{\text{syn}}}{\partial\delta m}\delta m\right)\Big/\frac{\partial V_{\text{syn}}}{\partial T}\to\min_T \qquad \text{at} \qquad T>T_{\text{sol}},$$

where $F_{\text{d}}=\frac{\pi a/2}{\tan(\pi a/2)}$ is the damping factor. The values $\frac{\partial V_{\text{syn}}}{\partial\delta m}$ are obtained experimentally (Sato et al., 1989), and δm is the degree of partial melting obtained from McKenzie and Bickle (1988). We used the solidus temperature T_{sol} of a dry peridotite (Takahashi, 1986). The laterally averaged temperature in the crust and mantle modeled by Demetrescu and Andreescu (1994) was chosen as the background temperature T_{bg} for the inversion of seismic velocity anomalies to temperature (see Fig. 3, Ismail-Zadeh et al., 2005a). The temperature in the shallow levels of the region is constrained from measured surface heat flux corrected for paleoclimate changes and for the effects of sedimentation (Demetrescu et al., 2001).

We note that the model of the present temperature by Ismail-Zadeh et al. (2005a) is based on the previous seismic-tomographic model of Martin et al. (2003), where the variations in crustal thickness were not considered in travel-time calculations. The seismic-tomographic model by Martin et al. (2006) is now used to convert the seismic velocity anomalies beneath the region into temperature.

Appendix B. Optimization problem for data assimilation

To assimilate the known temperature φ at $t=\vartheta$ (the input data on the present temperature) into the past, the following functional should be minimized with respect to the regularization parameter $\beta=\beta_k$:

$$J=\left\|T(t=\vartheta,\cdot;T_{\beta_k}(t=0,\cdot))-\varphi(\cdot)\right\|\to\min_k, \quad \beta_k=\beta_0 q^{k-1}, \quad k=1,2,\ldots,M,$$

where sign ||·|| denotes the norm in the Hilbert space $L_2(\Omega)$. Here $T_k=T_{\beta_k}(t=0,\cdot)$ is the solution (at time t=0) to the regularized backward heat Eq. (3) at the initial condition φ and the relevant boundary conditions; $T(t=\vartheta,\cdot;T_k)$ is the solution (at time $t=\vartheta$) to the heat equation

$$\partial T/\partial t+\mathbf{u}\cdot\nabla T=\nabla^2 T, \quad t\in[0,\vartheta], \quad \mathbf{x}\in\Omega$$

at the initial condition $T(t=0,\cdot)=T_k$ and the relevant boundary conditions; small parameters $\beta_0>0$, and $0<q<1$. When q tends to unity, the computational cost becomes large; and when q tends to zero, the optimal solution can be missed.

If the functional J does not exceed the predefined accuracy $\delta>0$ at $k=m$, the minimization is terminated, and $T_m=T_{\beta_m}(t=0,\cdot)$ is considered as the initial temperature derived from the input temperature assimilated into the past. Otherwise, parameters β_0, q, and M are modified, and the minimization is continued.

References

Agee, C.B., 1993. Petrology of the mantle transition zone. Ann. Rev. Earth Planet. Sci. 21, 19–41.

Balla, Z., 1987. Tertiary paleomagnetic data for the Carpatho-Pannonian region in the light of Miocene rotation kinematics. Tectonophysics 139, 67–98.

Bass, J.D., 1995. Elasticity of minerals, glasses, and melts. In: Ahrens, T.J. (Ed.), Mineral Physics and Crystallography, A Handbook of Physical Constants. Amer. Geophys. Union, Washington, D.C., pp. 45–63.

Busse, F.H., Christensen, U., Clever, R., Cserepes, L., Gable, C., Giannandrea, E., Guillou, L., Houseman, G., Nataf, H.-C., Ogawa, M., Parmentier, M., Sotin, C., Travis, B., 1993. 3D convection at infinite Prandtl number in Cartesian geometry—a benchmark comparison. Geophys. Astrophys. Fluid Dyn. 75, 39–59.

Chen, W.-P., Brudzinski, M.R., 2001. Evidence for a large-scale remnant of subducted lithosphere beneath Fiji. Science 292, 2475–2479.

Cloetingh, S.A.P.L., Burov, E., Matenco, L., Toussaint, G., Bertotti, G., Andriessen, P.A.M., Wortel, M.J.R., Spakman, W., 2004. Thermo-mechanical controls on the model of continental collision in the SE Carpathians (Romania). Earth Planet. Sci. Lett. 218, 57–76.

Csontos, L., Nagymarosy, A., Horvath, F., Kovac, M., 1992. Tertiary evolution of the intra-Carpathian area; a model. Tectonophysics 208, 221–241.

Demetrescu, C., Andreescu, M., 1994. On the thermal regime of some tectonic units in a continental collision environment in Romania. Tectonophysics 230, 265–276.

Demetrescu, C., Nielsen, S.B., Ene, M., Serban, D.Z., Polonic, G., Andreescu, M., Pop, A., Balling, N., 2001. Lithosphere thermal structure and evolution of the Transylvanian Depression—insight from new geothermal measurements and modelling results. Phys. Earth Planet. Inter. 126, 249–267.

Dziewonski, A.M., Anderson, D.L., 1981. Preliminary Reference Earth Model (PREM). Phys. Earth Planet. Inter. 25, 297–356.

Engdahl, E.R., van der Hilst, R., Buland, R., 1998. Global teleseismic earthquake relocation with improved travel times and procedure for depth determination. Bull. Seism. Soc. Am. 88, 722–743.

Evans, J.R., Achauer, U., 1993. Teleseismic velocity tomography using the ACH-method: theory and application to continental-scale studies. In: Iyer, K.M., Hirahara, K. (Eds.), Seismic Tomography: Theory and Practise. Chapman & Hall, London, pp. 319–360.

Forte, A.M., Woodward, R.L., Dziewonski, A.M., 1994. Joint inversions of seismic and geodynamic data for models of three-dimensional mantle heterogeneity. J. Geophys. Res. 99, 21857–21887.

Forte, A.M., Dziewonski, A.M., O' Connell, R.J., 1995. Thermal and chemical heterogeneity in the mantle: a seismic and geodynamic study of continental roots. Phys. Earth Planet. Inter. 92, 45–55.

Fuchs, K., Bonjer, K., Bock, G., Cornea, I., Radu, C., Enescu, D., Jianu, D., Nourescu, A., Merkler, G., Moldoveanu, T., Tudorache, G., 1979. The Romanian earthquake of March 4, 1977. II. Aftershocks and migration of seismic activity. Tectonophysics 53, 225–247.
Fügenschuh, B., Schmid, S.M., 2005. Age and significance of core complex formation in a very curved orogen: evidence from fission track studies in the South Carpathians (Romania). Tectonophysics 404, 33–53.
Girbacea, R., Frisch, W., 1998. Slab in the wrong place: lower lithospheric mantle delamination in the last stage of the Eastern Carpathian subduction retreat. Geology 26, 611–614.
Goes, S., Govers, R., Vacher, P., 2000. Shallow mantle temperatures under Europe from P and S wave tomography. J. Geophys. Res. 105, 11153–11169.
Green, D.H., Falloon, T.J., 1998. Pyrolite: a Ringwood concept and its current expression. In: Jackson, I. (Ed.), The Earth's Mantle. Cambridge University Press, Cambridge, pp. 311–378.
Green II, H.W., Burnley, P.C., 1989. A new self-organizing mechanism for deep-focus earthquakes. Nature 341, 733–737.
Griffin, W.L., O' Reilly, S.Y., Ryan, C.G., Gaul, O., Ionov, D.A., 1998. Secular variation in the composition of subcontinental lithospheric mantle: geophysical and geodynamic implications. In: Braun, J., et al. (Ed.), Structure and Evolution of the Australian Continent. Amer. Geophys. Union, Geodyn. Ser., vol. 26, pp. 1–26. Washington, D.C.
Griggs, D.T., Baker, D.W., 1969. The origin of deep-focus earthquakes. In: Mark, H., Fernbach, S. (Eds.), Properties of Matter Under Unusual Conditions. Wiley, New York, pp. 23–42.
Gvirtzman, Z., 2002. Partial detachment of a lithospheric root under the southeast Carpathians: toward a better definition of the detachment concept. Geology 30, 51–54.
Hacker, B.R., Peacock, S.M., Abers, G.A., Holloway, S.D., 2003. Subduction factory. 2. Are intermediate-depth earthquakes in subducting slabs linked to metamorphic dehydration reactions? J. Geophys. Res. 108. doi:10.1029/ 2001JB001129.
Hamilton, R.S., 1982. Three manifolds with positive Ricci curvature. J. Diff. Geom. 17, 255–306.
Honda, S., Morishige, M., Orihashi, Y., 2007. Sinking hot anomaly trapped at the 410 km discontinuity near the Honshu subduction zone, Japan. Earth Planet. Sci. Lett. 261, 565–577.
Ismail-Zadeh, A.T., Korotkii, A.I., Tsepelev, I.A., 2003. Numerical approach to solving problems of slow viscous flow backwards in time. In: Bathe, K.J. (Ed.), Computational Fluid and Solid Mechanics. Elsevier Science, Amsterdam, pp. 938–941.
Ismail-Zadeh, A., Mueller, B., Schubert, G., 2005a. Three-dimensional modeling of present-day tectonic stress beneath the earthquake-prone southeastern Carpathians based on integrated analysis of seismic, heat flow, and gravity observations. Phys. Earth Planet. Inter. 149, 81–98.
Ismail-Zadeh, A., Mueller, B., Wenzel, F., 2005b. Modelling of descending slab evolution beneath the SE-Carpathians: implications for seismicity. In: Wenzel, F. (Ed.), Perspectives in Modern Seismology. Lecture Notes in Earth Sciences, vol. 105. Springer-Verlag, Heidelberg, pp. 205–226.
Ismail-Zadeh, A.T., Panza, G.F., Naimark, B.M., 2000. Stress in the descending relic slab beneath the Vrancea region, Romania. Pure Appl. Geophys. 157, 111–130.
Ismail-Zadeh, A.T., Korotkii, A.I., Naimark, B.M., Tsepelev, I.A., 2001. Numerical modelling of three-dimensional viscous flow under gravity and thermal effects. Comput. Math. Math. Phys. 41 (9), 1331–1345.
Ismail-Zadeh, A., Korotkii, A., Schubert, G., Tsepelev, I., 2007. Quasi-reversibility method for data assimilation in models of mantle dynamics. Geophys. J. Int. 170, 1381–1398.
Ismail-Zadeh, A., Schubert, G., Tsepelev, I., Korotkii, A., 2004. Inverse problem of thermal convection: numerical approach and application to mantle plume restoration. Phys. Earth Planet. Inter. 145, 99–114.
Ismail-Zadeh, A., Schubert, G., Tsepelev, I., Korotkii, A., 2006. Three-dimensional forward and backward numerical modeling of mantle plume evolution: effects of thermal diffusion. J. Geophys. Res. 111, B06401. doi:10.1029/2005JB003782.
Jiricek, R., 1979. Tectonic development of the Carpathian arc in the Oligocene and Neogene. In: Mahel, M. (Ed.), Tectonic Profiles Through the Western Carpathians. Geol. Inst., Dionyz Stur, pp. 205–214.
Kanamori, H., Anderson, D.L., 1977. Importance of physical dispersion in surface-wave and free-oscillation problems—review. Rev. Geophys. Space Phys. 15, 105–112.
Karato, S.-I., 1993. Importance of anelasticity in the interpretation of seismic tomography. Geophys. Res. Lett. 20, 1623–1626.
Karato, S.-I., 2004. Mapping water content in the upper mantle. In: Eiler, J. (Ed.), Inside the Subduction Factory. Amer. Geophys. Union, Geophys. Monogr. Ser. 138, Washington, D.C., pp. 135–152.
Katsura, T., Yamada, H., Nishikawa, O., Song, M., Kubo, A., Shinmei, T., Yokoshi, S., Aizawa, Y., Yoshino, T., Walter, M.J., Ito, E., Funakoshi, K., 2004. Olivine–wadsleyite transition in the system (Mg, Fe)$_2$SiO$_4$. J. Geophys. Res. 109, B02209. doi:10.1029/2003JB002438.
Kennett, B.L.N., Engdahl, E.R., 1991. Travel times for global earthquake locations and phase identification. Geophys. J. Int. 105, 429–465.
Knapp, J.H., Knapp, C.C., Raileanu, V., Matence, L., Mocanu, V., Dinu, C., 2005. Crustal constraints on the origin of mantle seismicity in the Vrancea Zone, Romania: the case for active continental lithospheric delamination. Tectonophysics 410, 311–323.
Linzer, H.-G., 1996. Kinematics of retreating subduction along the Carpathian arc, Romania. Geology 24, 167–170.
Martin, M., the CALIXTO working group, 2003. High resolution teleseismic P-wave tomography for SE-Romania. Geophys. Res. Abst. 5, 10512.
Martin, M., Ritter, J.R.R., the CALIXTO working group, 2005. High-resolution teleseismic body-wave tomography beneath SE Romania—I. Implications for three-dimensional versus one-dimensional crustal correction strategies with a new crustal velocity model. Geophys. J. Int. 162, 448–460.
Martin, M., Wenzel, F., the CALIXTO working group, 2006. High-resolution teleseismic body wave tomography beneath SE-Romania—II. Imaging of a slab detachment scenario: Geophys. J. Int. 164, 579–595.
Matenco, L., Bertotti, G., Leever, K., Cloetingh, S., Schmid, S.M., Tarapoanca, M., Dinu, C., 2007. Large-scale deformation in a locked collisional boundary: interplay between subsidence and uplift, intraplate stress, and inherited lithospheric structure in the late stage of the SE Carpathians evolution. Tectonics 26, TC4011. doi:10.1029/2006TC001951.
McKenzie, D.P., 1972. Active tectonics of the Mediterranean region. Geophys. J. Roy. Astr. Soc. 30, 109–185.
McKenzie, D.P., Bickle, M.J., 1988. The volume and composition of melt generated by extension of the lithosphere. J. Petrol. 29, 625–679.
Montagner, J.-P., Kennett, B.L.N., 1996. How to reconcile body-wave and normal-mode reference Earth models. Geophys. J. Int. 125, 229–248.
Morley, C.K., 1996. Models for relative motion of crustal blocks within the Carpathian region, based on restorations of the outer Carpathian thrust sheets. Tectonics 15, 885–904.
Morra, G., Regenauer-Lieb, K., Giardini, D., 2006. Curvature of oceanic arcs. Geology 34, 877–880.
Nitoi, E., Munteanu, M., Marincea, S., Paraschivoiu, V., 2002. Magma–enclave interactions in the East Carpathian Subvolcanic Zone, Romania: petrogenetic implications. J. Volcanol. Geotherm. Res. 118, 229–259.
Oncescu, M.C., 1984. Deep structure of the Vrancea region, Romania, inferred from simultaneous inversion for hypocentres and 3-D velocity structure. Ann. Geophys. 2, 23–28.
Oncescu, M.C., Bonjer, K.P., 1997. A note on the depth recurrence and strain release of large Vrancea earthquakes. Tectonophysics 272, 291–302.
Pana, D., Erdmer, P., 1996. Kinematics of retreating subduction along the Carpathian arc, Romania. Comment. Geology 24, 862–863.
Pana, D., Morris, G.A., 1999. Slab in the wrong place: Lower lithospheric mantle delamination in the last stage of the Eastern Carpathian subduction retreat: Comment. Geology 27, 665–666.
Perelman, G., 2002. The Entropy Formula for the Ricci Flow and its Geometric Applications. http://arxiv.org/abs/math.DG/0211159.
Popa, M., Radulian, M., Grecu, B., Popescu, E., Placinta, A.O., 2005. Attenuation in Southeastern Carpathians area: result of upper mantle inhomogeneity. Tectonophysics 410, 235–249.
Roure, F., Roca, E., Sassi, W., 1993. The Neogene evolution of the Outer Carpathian Flysch units (Poland, Ukraine and Romania): kinematics of a foreland/fold-and-thrust belt system. Sediment. Geol. 86, 177–201.
Royden, L.H., 1988. Late Cenozoic tectonics of the Pannonian basin system. Am. Assoc. Pet. Geol. Mem. 45, 27–48.
Sandulescu, M., 1988. Cenozoic tectonic history of the Carpathians. Am. Assoc. Pet. Geol. Mem. 45, 17–25.
Sato, H., Sacks, I.S., Murase, T., Muncill, G., Fukuyama, H., 1989. QP-melting temperature relation in peridotite at high pressure and temperature: attenuation mechanism and implications for the mechanical properties of the upper mantle. J. Geophys. Res. 94, 10647–10661.
Seghedi, I., Downes, H., Vaselli, O., Szakacs, A., Balogh, K., Pecskay, Z., 2004. Post-collisional Tertiary–Quaternary mafic alkalic magmatism in the Carpathian–Pannonian region: a review. Tectonophysics 393, 43–62.
Sperner, B., the CRC 461 Team, 2005. Monitoring of slab detachment in the Carpathians. In: Wenzel, F. (Ed.), Challenges for Earth Sciences in the 21st Century. Springer-Verlag, Heidelberg, pp. 187–202.
Sperner, B., Lorenz, F., Bonjer, K., Hettel, S., Müller, B., Wenzel, F., 2001. Slab break-off—abrupt cut or gradual detachment? New insights from the Vrancea region (SE Carpathians, Romania). Terra Nova 13, 172–179.
Stanica, D., Stanica, M., 1993. An electrical resistivity lithospheric model in the Carpathian orogen from Romania. Phys. Earth Planet. Inter. 81, 99–105.
Szabo, C., Falus, G., Zajacz, Z., Kovacs, I., Bali, E., 2004. Composition and evolution of lithosphere beneath the Carpathian–Pannonian Region: a review. Tectonophysics 393, 119–137.
Takahashi, E., 1986. Melting of a dry peridotite KLB-1 up to 14 GPa: implications on the origin of peridotitic upper mantle. J. Geophys. Res. 91, 9367–9382.
Tarapoanca, M., Carcia-Catellanos, D., Bertotti, G., Matenco, L., Cloetingh, S.A.P.L., Dinu, C., 2004. Role of the 3-D distributions of load and lithospheric strength in orogenic arcs: polystage subsidence in the Carpathians foredeep. Earth Planet. Sci. Lett. 221, 163–180.
Trushkov, V.V., 2002. An example of (3+1)-dimensional integrable system. Acta Appl. Math. 72 (1–2), 111–122.
Weidle, C., Wenzel, F., Ismail-Zadeh, A., 2007. t*—an unsuitable parameter for anelastic attenuation in the Eastern Carpathians. Geophys. J. Int. 170, 1139–1150.
Wenzel, F., Lorenz, F.P., Sperner, B., Oncescu, M.C., 1999. Seismotectonics of the Romanian Vrancea area. In: Wenzel, F., Lungu, D., Novak, O. (Eds.), Vrancea Earthquakes: Tectonics, Hazard and Risk Mitigation. Kluwer Publishers, Dordrecht, pp. 15–25.
Wortel, M.J.R., Spakman, W., 2000. Subduction and slab detachment in the Mediterranean–Carpathian region. Science 290, 1910–1917.